



Supplement of

Observations of gas-phase products from the nitrate-radical-initiated oxidation of four monoterpenes

Michelia Dam et al.

Correspondence to: James N. Smith (jimsmith@uci.edu)

The copyright of individual parts of the supplement might differ from the article licence.

S1 KinSim model rate constants and results

Summary of rate constants used for the model are shown in Table S1 and results for the a-pinene and b-pinene systems are shown in Figure S1. Most come from the JPL Kinetics Data Evaluation (JPL 2015) or the IUPAC Evaluated kinetic and photochemical data for atmospheric chemistry (IUPAC 2006). The rate constants for a-thujene have not been measured and therefore, the a-thujene system was not modeled.

Table S1. Table of rate constants used for modeling experiments.

Rate Constants Used for KinSim Modeling					
reactant	reactant	product	product	k (s-1)	source
NO	O3	NO2	O2	1.96E-14	JPL
NO2	O3	NO3	O2	5.70E-17	JPL
NO2	NO3	N2O5		1.24E-12	JPL
N2O5		NO3	NO2	0.0445	IUPAC
NO	NO3	NO2	NO2	2.60E-11	DeMore et al. 1994
NO3	MT	RO2		(dcar) 9.1E-12 (bpin) 2.5E-12 (apin) 6.2E-12	Ng et al. 2017 & Calvert et al. 2002
O3	MT	ProdO3MT		(dcar) 3.70E-17 (bpin) 2.25E-17 (apin) 8.00E-17	Khamaganov et al. 2001
N2O5	H2O	HNO3	HNO3	9.67E-05	
DILUTION1				0.0006	
O3source		O3		0.0006	
MTsource		MT		0.0006	
NO2source		NO2		0.0006	
N2O5		N2O5wall		0.00125	Measured
NO3		NO3wall		0.0104	
RO2	RO2	PRO2RO2		2.00E-15	Ziemann and Atkinson 2012
RO2	NO3	PRO2NO3		2.00E-12	Orlando and Tyndall 2012
RO2	NO2	RO2NO2		2.00E-12	JPL
RO2NO2		RO2	NO2	3.60	
RO2NO2		RO2NO2wall		0.00125	

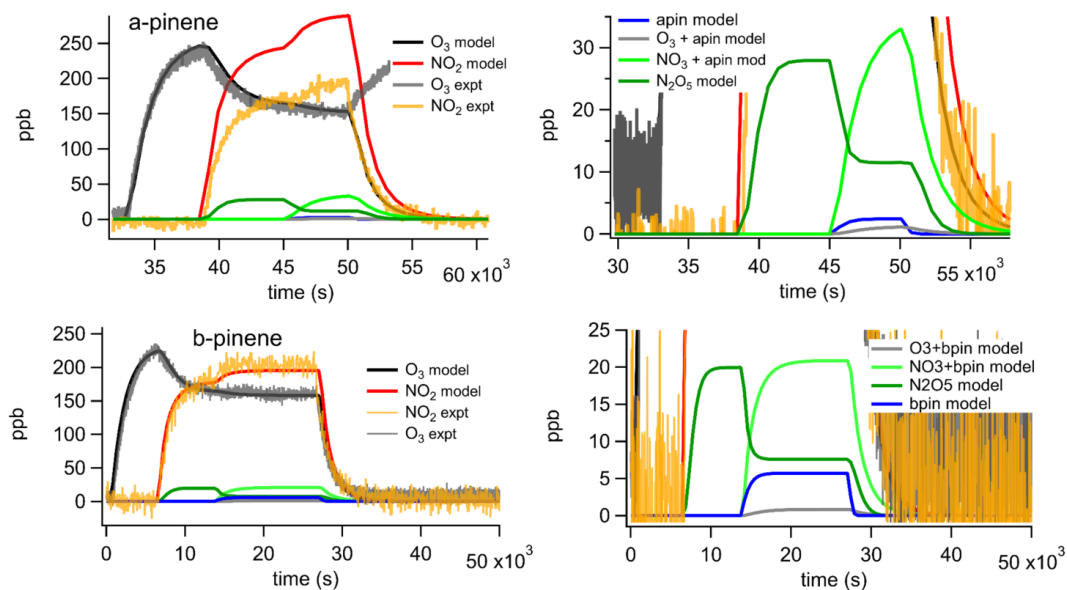


Figure S1. KinSim model results for the a-pinene and b-pinene systems. For the a-pinene system, initial modeled NO_2 concentration was made to match experimental NO_2 , but magnitude was scaled to make modeled O_3 fit experimental O_3 because the magnitude of the O_3 measurement was more reliable.

S2 Monoterpene chemical information

(-)-beta-pinene >94.0% purity, TCI Chemicals, CAS 18172-67-3.

(+)-3-carene >90.0% purity, TCI Chemicals, CAS 13466-78-9.

(+)-alpha-pinene 98% purity, Sigma Aldrich, LOT SHBH5409V.

- 5 alpha-thujene: We isolated alpha-thujene by fractional distillation of commercially-available *Boswellia serrata* (frankincense) essential oil. We kept the temperature of the distilling flask at 175 C and collected 5 mL of the vapors that were first to condense. We then repeated the process 2 more times to get a small sample of triple-distilled oil. We estimated the composition of the sample by running GC-MS. The sample was 93% a-thujene in July 2019 and 91% in November 2019, so we are assuming the sample was >90% pure when we ran the chamber experiments. The most significant impurity is a-pinene. The frankincense
- 10 oil we used was about 65% a-thujene prior to distillation. For GC analysis, we used a Varian Saturn GCMS with a Restek dimethyl polysiloxane 30 m column and ether as the solvent. Initial oven temperature was 50 C, then ramp to 200 C at 10 C/min for 15 minutes.

S3 Particle size distributions

Size distributions of each MT system were measured using an SMPS system. New particle formation was observed for the d-carene and b-pinene systems and no particle formation was observed for the a-thujene and a-pinene systems.

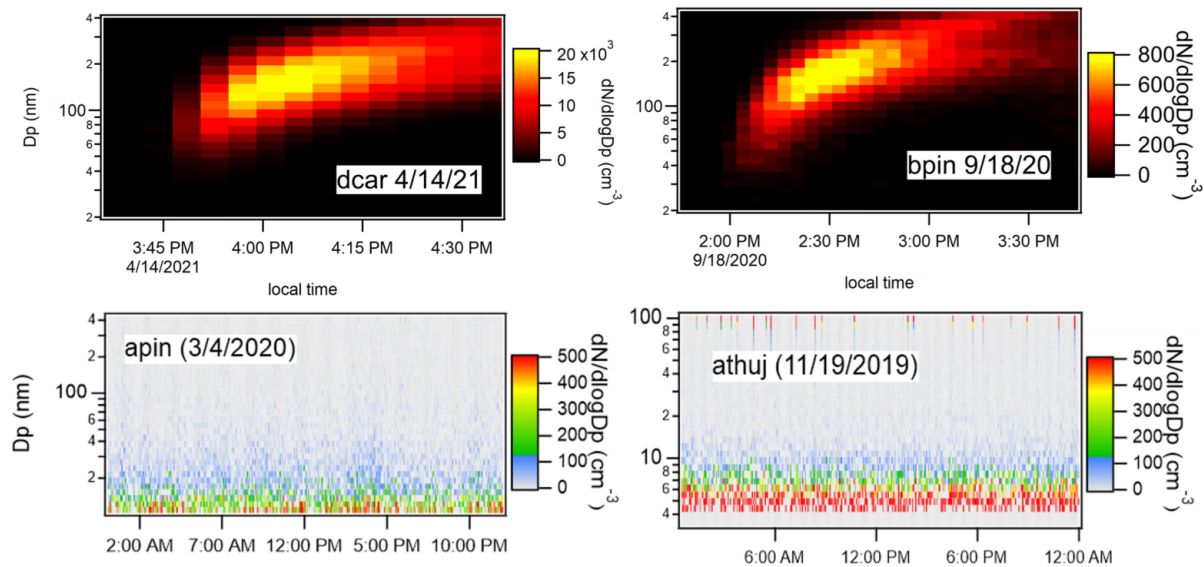


Figure S2. Particle size distributions of each MT system.

S4 CIMS yield processing

Peaks were fit and integrated using Tofware. Equation (1) details the yield calculation. The integrated signals for every peak were summed, divided by the reagent ion (NO_3^- , multiplied by the calibration factor ($F_{cal} = 6 \times 10^{10}$), averaged over the duration of the experiment to find the raw number of molecules generated. That number was multiplied by the wall loss correction factor (Fcor) for monomers (1.29) and dimers (1.49) separately, then multiplied by the flow rate going into the inlet of the mass spec to find molecules cm^{-3} .

$$\frac{\frac{\sum_{int}^{NO_3^-} \times F_{cal}}{time}}{\times F_{cor}} \times flow^{-1} = cm^{-3} \quad (1)$$

S5 Detailed mechanisms for each MT system

Mechanisms for each MT system are shown in this section. "X" corresponds to bimolecular reactions with nighttime radicals (NO_3 , HO_2 , RO_2). Blue arrows indicated alkoxy scission pathways and red arrows indicate alkyl radical rearrangement ring opening reactions. ROOR indicate dimerization reactions and EP indicate RO_2 epoxide forming reactions.

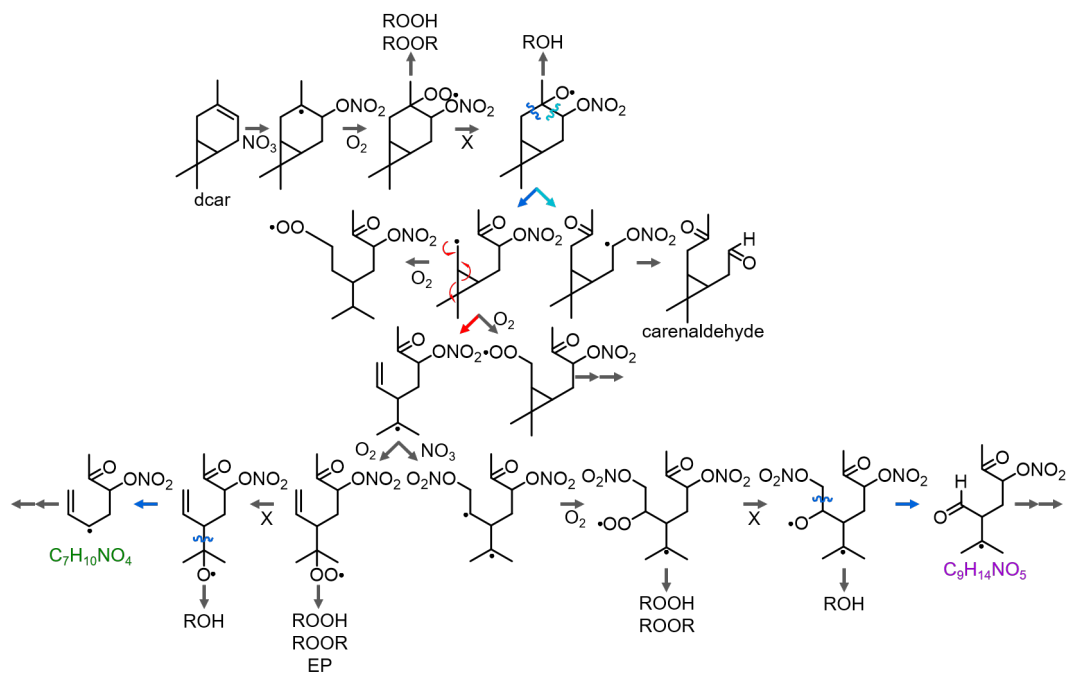


Figure S3. Detailed NO_3 + d-carene mechanism scheme.

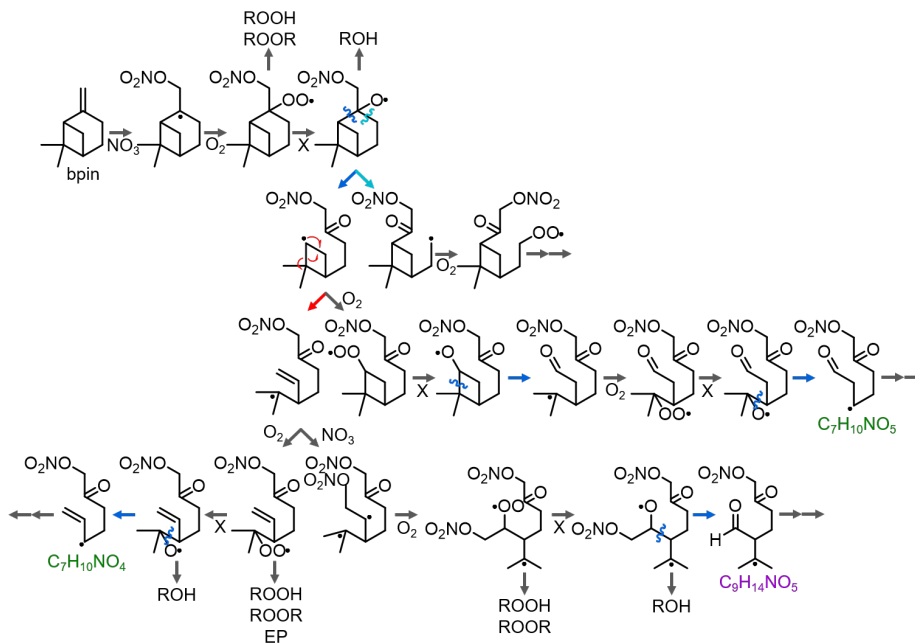


Figure S4. Detailed NO₃ b-pinene mechanism scheme.

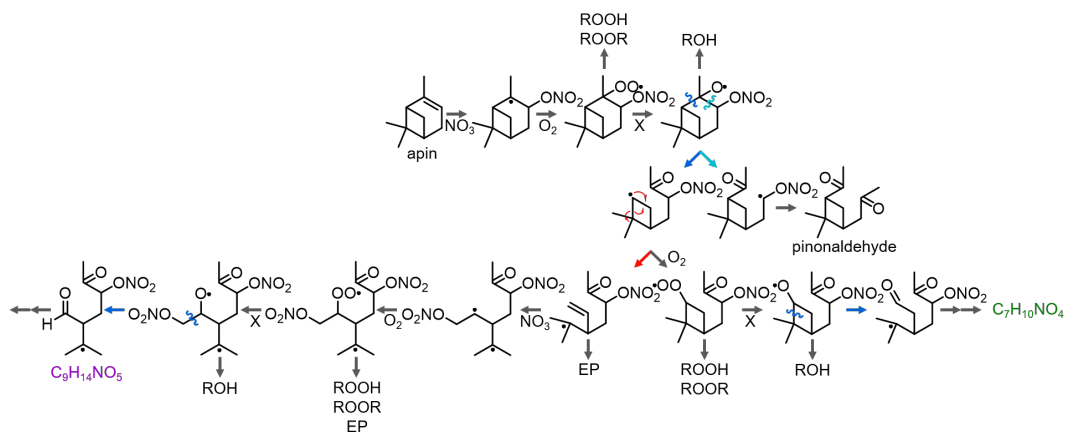


Figure S5. Detailed NO₃ a-pinene mechanism scheme.

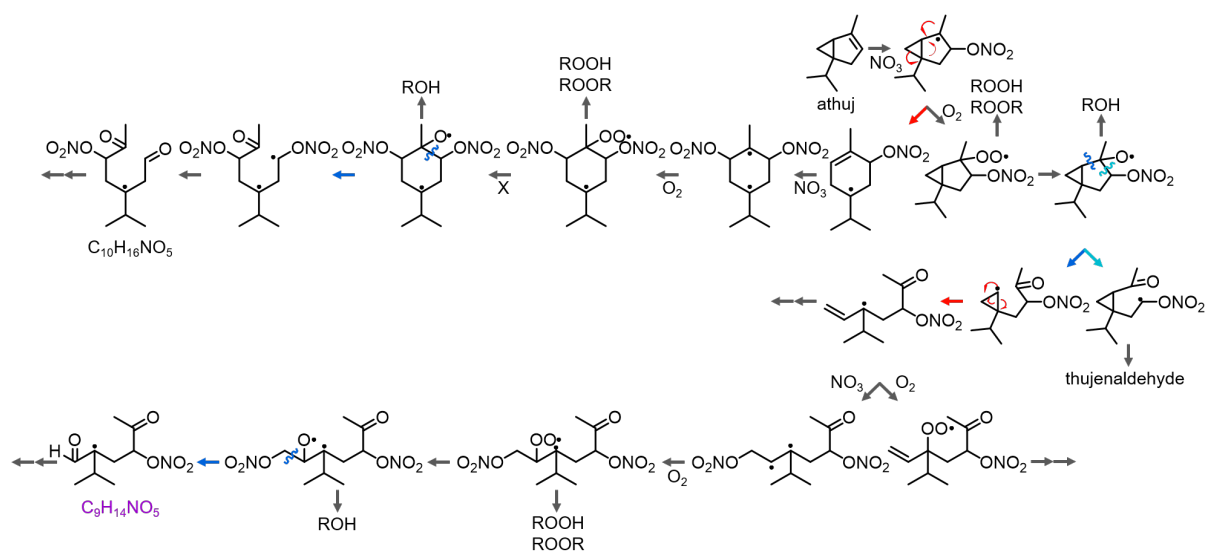


Figure S6. Detailed NO₃ a-thujene mechanism scheme.

S6 Wall loss of N₂O₅ and dcar + NO₃ products

N₂O₅ was measured using I-CIMS with the same inlet configuration (TI) used for NO₃-CIMS. I⁻ ion was produced by filling a teflon permeation cell with liquid methyl iodide and flowing ultrahigh purity N₂ over a sealed stainless steel canister containing the permeation cell. I⁻, I₂⁻, IN₂O₅, and IHNO₃ were used as calibration ions. Peaks were analyzed using tofware in Igor. The decay of N₂O₅ was fitted to an exponential function and the k value was found to be $1.25 \times 10^{-3} \text{ s}^{-1}$.

Wall losses for individual species were measured for the dcar system by observing the time traces of ion abundance when the ion production term is zero and therefore the concentration of species A normalized by the initial concentration is determined by first order loss rates due to dilution (k_{dil}) and wall deposition (k_{dep}) as follows:

$$[A]/[A]_o = \exp[-(k_{dil} + k_{dep})t].$$

These conditions were created by allowing the gas phase species to reach steady state, then shutting off the oxidant and dcar flow into the chamber. The missing flow was made up with zero air in order to maintain a constant dilution rate. We used NO₂ to determine k_{dil} , since prior experiments using the same chamber reported a wall loss rate of this compound of 10^{-6} , about 3-4 orders of magnitude higher than wall loss rates observed for oxidation products in this study (DeHaan et al., 1999). The value of k_{dil} can thereby be taken from an exponential fit of the NO₂ data according to:

$$[NO_2]/[NO_2]_o = \exp(-k_{dil}t).$$

The wall loss rate for each species, A, can be calculated directly from the measurements by dividing the normalized NO₂ concentration by the normalized concentration of species A:

$$\frac{[NO_2]/[NO_2]_o}{[A]/[A]_o} = \frac{1}{\exp(-k_{dep}t)} = \exp(k_{dep}t).$$

Since the values of k_{dil} and k_{dep} are small compared to the time scales of these experiments, we can make the simplifying assumption that the exponential terms can be replaced by their Taylor expansion, i.e., $e^{-x} \approx 1 - x$. With this simplification, the ratio shown above can be replaced by linear terms as follows:

$$[NO_2]/[NO_2]_o - [A]/[A]_o = \exp(k_{dep}t).$$

Figure S7 shows an example of this analysis. The figure shows the normalized decay curves for NO₂ and a representative C₂₀ compound. It also shows the difference curve, to which we fit an exponential function in order to calculate k_{dep} . These values of k_{dep} for each detected species were used to correct the measured ion abundance for wall losses, as shown in the right plot of Figure S7. These traces were fitted to sigmoidal curves to find the net formation time of each individual compound, as shown in Figure S8. Overall, the net formation times were greatly affected by the wall correction. Shifts of up to one minute in the positive or negative direction were observed, but monomers tended to have positive shifts smaller in magnitude and dimers had larger shifts in both directions.

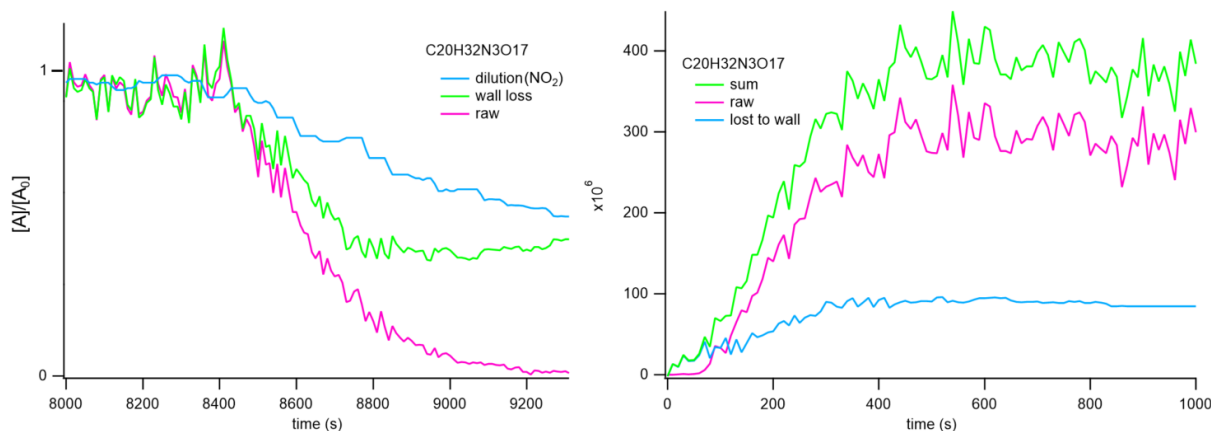


Figure S7. Manipulated time series trace of one species (C₂₀H₃₂N₂O₁₄ without reagent ion) as an example of how wall losses are calculated and formation times corrected.

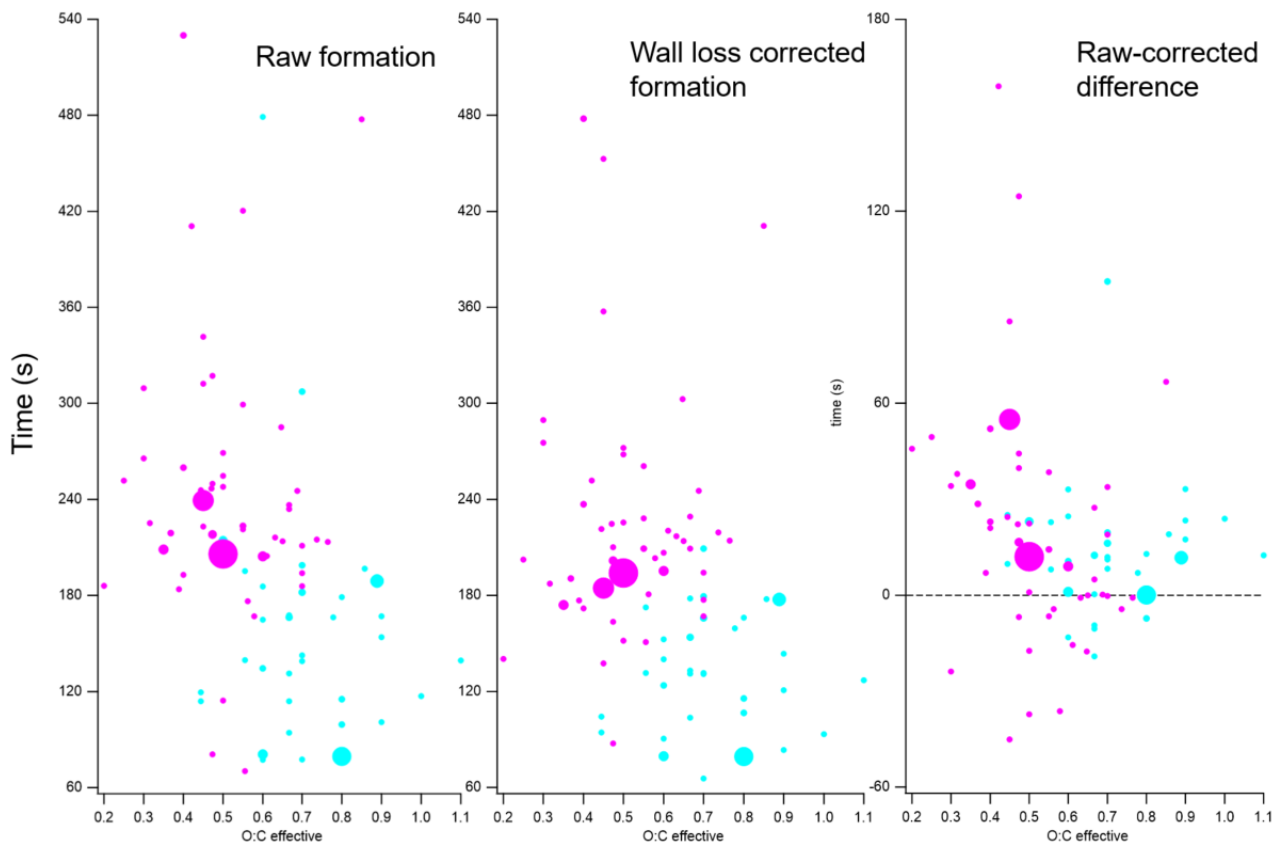


Figure S8. Speciated wall loss correction times for d-carene + NO₃ oxidation products plotted against O:C effective. Blue circles are monomer species and pink circles are dimer species.

Chamber mixing was characterized by performing experiments measuring CO₂. Experiments were conducted at 20 LPM inlet flow with CO₂ added to the chamber. Following this we flushed the chamber with CO₂-scrubbed zero air. A Licor CO₂ analyzer measured CO₂ concentration. Figure S9 shows the results along with the best fit line for the decay of CO₂. We then fit the data to an exponential equation for dilution in a continuously stirred chamber in order to calculate the average residence time at this flow rate. The result at this flow rate, 1657 s, is to be compared to the theoretical residence time associated with a well-mixed chamber of 1680 s. This close correspondence is found at flow rates ranging from 10 - 60 lpm and confirms that our use of Teflon “shower heads” to introduce gasses into the chamber creates satisfactory mixing in the chamber.

The mixing time for our experiments is approximately 100 s. This value arises from experiments performed in which a pulse of CO₂ was introduced into the chamber at $t = 0$ s, after which we observed the mixing process and decay of CO₂. Figure S10 shows that it takes ~ 100 s for the CO₂ to reach its peak value, which is equal to the theoretically predicted value based on the concentration of CO₂ added and the dilution ratio.

Characterization of residence time

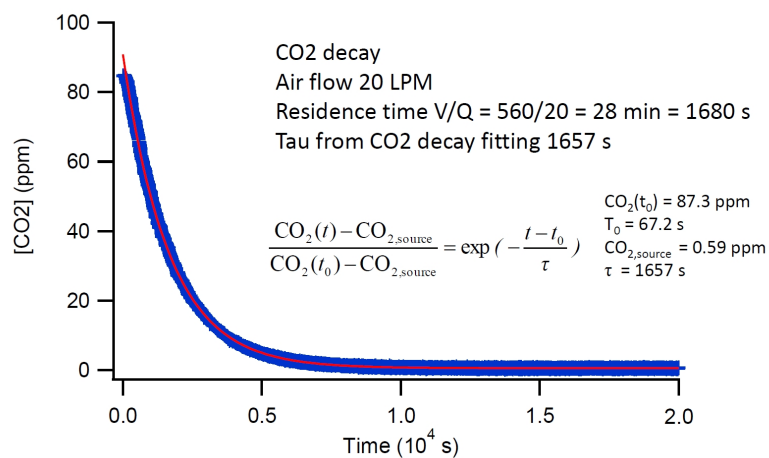


Figure S9. Comparison of experimentally determined residence time to that calculated assuming a well-mixed chamber.

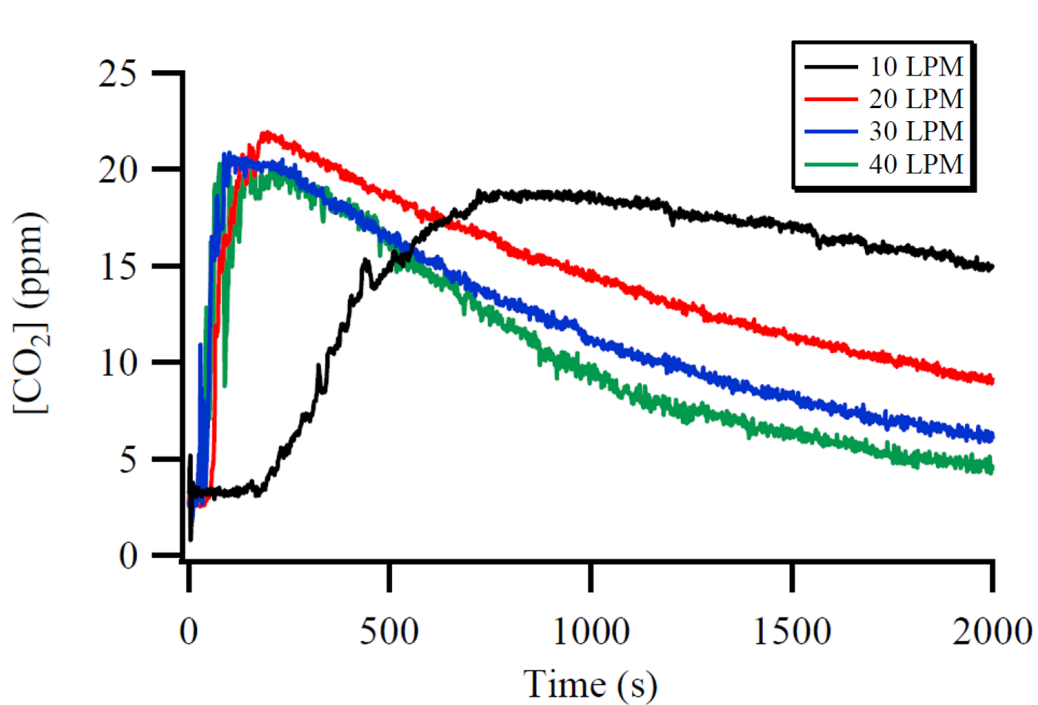


Figure S10. Measurements of [CO₂] exiting chamber after a pulse of CO₂ was added at t=0.

S7 β -pinene experiments comparison of results from high and low concentration

- β -pinene + NO₃ experiments were done for two different concentrations of β -pinene, 8 and 80 ppb. Results from these experiments were averaged for comparison to the other MT systems, but raw results from each experiment are shown in this section (Figure S11). The mass spectra for these two experiments were very similar. Almost every major peak was present in both spectra. However, elemental ratios for each experiment show changes in every category, with major changes observed for fragmentation and oligomerization products (C number). About 10% more C₇ fragments and 10% less C₁₀ species were observed for the high concentration experiments. Additionally, about 20% more C₂₀ dimer products were observed for the high concentration experiments, while the low concentration dimer carbon number distribution was more spread out among the C₁₇C₁₉ and C₂₀ peaks. Less drastic differences were observed for the other categories. Slightly more monomers (3%) than dimers and C₁₀N₂ than C₁₀N₁ products were formed in the low concentration experiment. Slightly more C₁₀N₁H₁₅ compounds than C₁₀N₁H₁₆ were measured for the high concentration experiment, as apposed to the low concentration experiment in which the H₁₆ and H₁₅ contributions are almost equal.

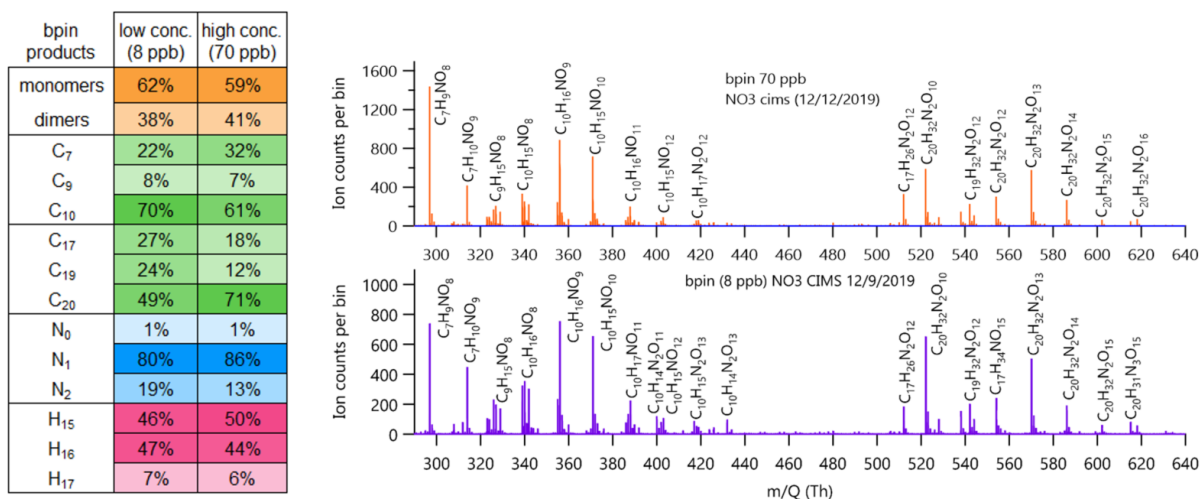


Figure S11. Comparison of elemental ratios and mass spectra for low concentration (8 ppb) and high concentration (70 ppb) bpin experiments.

S8 NO3-CIMS peak lists

d-carene peak list														
HR Peak ID (NO ₃ - cluster)	m/Q	normalized intensity	HR Peak ID (NO ₃ - cluster)	m/Q	normalized intensity	HR Peak ID (NO ₃ - cluster)	m/Q	normalized intensity	HR Peak ID (NO ₃ - cluster)	m/Q	normalized intensity	HR Peak ID (NO ₃ - cluster)	m/Q	normalized intensity
NO3	61.988	6.00E+10	C10H15N2O14	387.052	1.31E+07	C7H10N3O11	312.032	3.66E+06	C19H30N2O15	526.165	1.35E+06	C16H26N3O15	500.136	2.70E+05
HN2O6	124.983	2.25E+10	C19H15NO12	449.059	1.23E+07	C20H31N2O14	523.178	3.66E+06	C19H29N4O17	585.153	1.35E+06	C17H28N3O15	514.152	2.15E+05
C20H32N3O17	586.173	3.53E+08	H2N3O9	187.979	1.22E+07	C18H28N3O16	542.147	3.63E+06	C20H31N2O13	507.183	1.35E+06	C19H29N4O22	665.127	1.92E+05
C20H32N3O16	570.178	2.73E+08	C20H33N4O20	649.169	1.14E+07	C10H17N2O14	389.068	3.45E+06	C18H30N3O14	512.173	1.34E+06	C18H30N3O13	496.178	1.73E+05
C10H16N2O13	372.065	2.70E+08	C9H16N3O13	374.068	1.10E+07	C20H31N3O18	601.160	3.35E+06	C17H26N4O15	526.139	1.28E+06			
C9H14N3O15	404.042	2.30E+08	C20H32N3O21	650.153	1.10E+07	C20H32N5O20	662.164	3.30E+06	C16H24N3O16	514.116	1.24E+06			
C20H32N3O19	618.163	1.53E+08	C9H13N2O10	309.057	1.04E+07	C10H14NO9	292.067	3.19E+06	C18H30N4O17	574.161	1.22E+06			
C10H16N2O11	340.075	1.43E+08	C18H28N4O17	572.145	1.01E+07	C10H15N3O12	369.066	3.19E+06	C20H32N4O19	632.166	1.22E+06			
C20H32N3O14	538.188	1.40E+08	C20H32N2O17	558.167	9.91E+06	C10H16N3O17	450.048	3.19E+06	C18H30N3O18	576.152	1.21E+06			
C10H15N2O10	323.073	1.27E+08	C20H32N3O20	634.158	9.58E+06	C18H28N2O17	544.139	3.01E+06	C20H32N5O21	678.159	1.19E+06			
C19H30N3O16	556.163	1.09E+08	C20H31N4O20	647.153	9.55E+06	C19H30N3O13	508.178	2.99E+06	C19H32N3O18	590.168	1.11E+06			
C10H17N2O12	357.078	7.06E+07	C9H15N2O12	343.062	9.45E+06	C20H32N2O15	540.180	2.96E+06	C20H31N4O21	663.148	1.07E+06			
C9H13N2O11	325.052	7.00E+07	C10H16N3O14	402.063	8.65E+06	C9H12NO9	278.051	2.94E+06	C17H26N4O18	574.124	1.02E+06			
C10H16N3O15	418.058	5.77E+07	C20H31N4O18	615.163	8.24E+06	C20H32N3O13	522.194	2.88E+06	C16H24N3O18	546.105	1.02E+06			
C20H31N4O17	599.168	5.28E+07	C7H11N2O11	299.036	8.21E+06	C17H26N3O15	512.136	2.63E+06	C19H29N4O16	569.158	9.55E+05			
C20H32N3O15	554.183	5.05E+07	C10H16N2O14	388.060	6.59E+06	C20H33N2O17	559.175	2.46E+06	C18H28N3O13	494.162	8.50E+05			
C10H15N2O12	355.062	4.61E+07	C19H13NO12	447.044	6.18E+06	C15H22N3O17	516.095	2.40E+06	C19H29N3O21	635.129	8.47E+05			
C10H17N2O13	373.073	4.35E+07	C9H15N2O11	327.068	6.08E+06	C19H32N3O19	606.163	2.39E+06	C10H17N3O12	371.081	7.73E+05			
C20H32N3O18	602.168	3.81E+07	C20H32N2O17	572.170	5.95E+06	C20H31N4O15	567.179	2.33E+06	C18H28N3O19	590.132	7.55E+05			
C10H16N3O13	386.068	3.01E+07	C9H15N2O9	295.078	5.74E+06	C20H30N3O19	616.147	2.13E+06	C20H30N3O20	632.142	7.55E+05			
C10H15N3O14	401.055	2.83E+07	C9H12NO8	262.056	5.18E+06	C20H32N3O12	506.199	2.11E+06	C16H24N4O19	576.103	7.47E+05			
C19H30N3O14	524.173	2.65E+07	C9H13N2O9	293.062	4.97E+06	C17H26N3O18	560.121	2.09E+06	C20H33N4O21	665.164	7.47E+05			
C10H14N3O13	384.053	2.12E+07	C20H33N4O19	633.174	4.79E+06	C20H33N4O15	569.194	1.98E+06	C19H32N2O16	544.175	7.18E+05			
C10H16NO9	294.083	2.04E+07	C10H16N3O12	370.073	4.71E+06	C20H31N4O16	583.174	1.76E+06	C20H32N3O22	666.148	6.13E+05			
C10H16N2O12	356.070	1.80E+07	C20H32N3O11	490.204	4.40E+06	C19H32N3O15	542.183	1.70E+06	C20H33N2O12	493.203	5.64E+05			
C10H15N2O13	371.057	1.60E+07	C19H29N2O14	509.162	4.20E+06	C10H16N2O9	308.086	1.58E+06	C20H33N4O22	681.159	5.18E+05			
C10H15N2O11	339.068	1.59E+07	C10H14NO10	308.062	4.09E+06	C20H33N4O16	585.189	1.49E+06	C17H26N3O14	496.141	5.15E+05			
C10H17N3O14	403.071	1.51E+07	C19H31N4O15	555.179	3.99E+06	C19H30N3O21	636.137	1.45E+06	C15H22N3O16	500.100	5.05E+05			
C9H14N2O11	326.060	1.48E+07	C10H16N2O16	420.050	3.97E+06	C20H30N3O15	552.168	1.39E+06	C19H31NO16	529.164	5.00E+05			
C20H33N4O18	617.179	1.46E+07	C20H31N4O19	631.158	3.97E+06	C20H31N4O22	679.143	1.38E+06	C19H27N3O21	633.114	4.25E+05			
C19H30N3O19	604.147	1.45E+07	C20H30N3O17	584.158	3.94E+06	C19H30N2O14	510.170	1.38E+06	C18H30N3O17	560.158	3.45E+05			
C20H33N4O17	601.184	1.45E+07	C10H15N3O13	385.060	3.76E+06	C18H30N4O19	606.150	1.37E+06	C19H29N2O13	493.167	3.24E+05			

β-pinene peak list

HR Peak ID (NO ₃ - cluster)	m/Q	normalized intensity	HR Peak ID (NO ₃ - cluster)	m/Q	normalized intensity	HR Peak ID (NO ₃ - cluster)	m/Q	normalized intensity	HR Peak ID (NO ₃ - cluster)	m/Q	normalized intensity
NO3	61.988	6.00E+10	C20H32N3O18	602.168	5.44E+06	C9H15N3O11	341.071	1.54E+06	C9H11N2O10	307.041	5.15E+05
HN2O6	124.983	1.95E+10	C7H10N3O14	360.016	5.03E+06	C20H33N3O19	619.171	1.49E+06	C20H33N2O15	541.188	4.95E+05
C7H9N2O11	297.021	8.98E+07	C10H17N3O15	419.066	4.39E+06	C20H33N3O18	603.176	1.43E+06	C9H13N2O9	293.062	4.91E+05
C10H16N2O12	356.070	5.76E+07	C10H16N3O13	386.068	4.19E+06	C9H16N2O12	344.070	1.43E+06	C9H6N2O12	333.992	4.87E+05
C10H15N2O13	371.057	4.95E+07	C20H31N4O18	615.163	4.11E+06	C19H32N3O16	558.178	1.30E+06	C9H15N2O13	359.057	4.71E+05
C20H32N3O16	570.178	4.87E+07	C10H16N3O15	418.058	3.87E+06	C7H10N2O14	346.013	1.27E+06	C10H13N2O11	337.052	4.59E+05
C20H32N3O13	522.194	4.79E+07	C10H16N3O14	402.063	3.73E+06	C20H24N4O11	496.144	1.23E+06	C10H16N3O11	354.078	4.35E+05
C7H10N2O12	314.023	2.68E+07	C10H16N3O12	370.073	3.48E+06	C10H14N3O12	368.058	1.21E+06	C10H17N2O15	405.063	3.96E+05
C17H26N3O15	512.136	2.67E+07	C10H17N2O13	373.073	3.26E+06	C10H16N2O16	420.050	1.18E+06	C9H16N3O13	374.068	3.40E+05
C20H32N3O15	554.183	2.53E+07	C9H13N2O11	325.052	3.13E+06	C20H32N2O15	540.180	1.17E+06	C10H14N09	292.067	2.79E+05
C20H32N3O17	586.173	2.27E+07	C10H16N2O13	372.065	3.09E+06	C7H10N3O11	312.032	1.14E+06	C10H15N3O13	385.060	2.79E+05
C10H15N2O11	339.068	2.20E+07	C19H32N3O13	510.194	2.96E+06	C10H17N4O17	465.059	1.10E+06	C19H31N3O16	557.170	2.77E+05
C19H32N3O15	542.183	1.85E+07	C10H14N3O14	400.048	2.79E+06	C19H29N2O15	525.157	1.02E+06	C10H16N09	294.083	2.73E+05
C10H15N2O12	355.062	1.68E+07	C19H32N3O14	526.188	2.69E+06	C20H33N2O17	573.178	1.00E+06	C19H30N5O17	600.164	2.58E+05
C10H16N2O11	340.075	1.43E+07	C10H14N3O16	432.037	2.63E+06	C20H30N3O16	568.163	9.30E+05	C19H29N2O16	541.152	2.40E+05
C9H15N2O11	327.068	1.36E+07	C17H26N3O13	480.147	2.50E+06	C20H32N3O20	634.158	9.30E+05	C10H15N3O12	369.066	2.32E+05
C10H16N2O14	388.060	1.31E+07	C20H32N3O12	506.199	2.44E+06	C20H31N4O17	599.168	9.14E+05	C9H12N09	278.051	1.96E+05
C20H32N3O14	538.188	1.22E+07	C17H26N3O19	576.116	2.03E+06	C10H16N2O15	404.055	8.90E+05	C9H12N08	262.056	1.15E+05
C17H35N2O16	523.199	1.16E+07	C20H32N2O17	572.170	1.99E+06	C9H13N2O10	309.057	8.86E+05			
C7H9N2O13	329.010	9.58E+06	C20H32N2O16	556.175	1.98E+06	C20H31N4O19	631.158	8.70E+05			
C17H26N3O17	544.126	8.98E+06	C9H14N2O12	342.055	1.96E+06	C9H15N2O9	295.078	8.17E+05			
C10H17N2O12	357.078	8.98E+06	C10H16N3O16	434.053	1.85E+06	C20H33N4O17	601.184	7.93E+05			
C17H26N3O16	528.131	7.49E+06	C19H29N2O13	493.167	1.83E+06	C10H14N3O13	384.053	7.65E+05			
C10H15N2O15	403.047	6.56E+06	C10H16NO13	358.062	1.79E+06	C10H14N3O15	416.042	7.61E+05			
C10H15N2O14	387.052	6.44E+06	C9H15N2O12	343.062	1.72E+06	C20H33N4O18	617.179	7.13E+05			
C10H15N2O10	323.073	6.12E+06	C20H33N4O16	585.189	1.67E+06	C10H15N3O14	401.055	7.05E+05			
C20H32N3O19	618.163	6.12E+06	C10H15N3O15	417.050	1.65E+06	C20H31N4O16	583.174	6.89E+05			
C10H16N2O10	324.080	6.04E+06	C19H32N3O17	574.173	1.61E+06	C10H17N2O14	389.068	5.80E+05			
C20H33N3O17	587.181	5.48E+06	C10H15N2O9	307.078	1.61E+06	C20H31N4O15	567.179	5.32E+05			

α -thujene peak list														
HR Peak ID (NO ₃ - cluster)	m/Q	normalized intensity	HR Peak ID (NO ₃ - cluster)	m/Q	normalized intensity	HR Peak ID (NO ₃ - cluster)	m/Q	normalized intensity	HR Peak ID (NO ₃ - cluster)	m/Q	normalized intensity	HR Peak ID (NO ₃ - cluster)	m/Q	normalized intensity
NO3	61.988	6.00E+10	C10H15N2O16	419.042	3.95E+06	C9H13N2O12	341.047	1.63E+06	C20H33NO16	543.180	9.95E+05	C10H14N3O15	416.042	5.67E+05
HN2O6	124.983	1.86E+10	C20H32N3O19	618.163	3.55E+06	C10H14NO9	292.067	1.59E+06	C9H14N2O14	374.045	9.91E+05	C9H16NO10	298.077	5.41E+05
H2N3O9	187.979	1.42E+07	C10H15N2O10	323.073	3.46E+06	C19H29N2O13	493.167	1.58E+06	C19H28NO16	526.141	9.88E+05	C17H26N3O19	576.116	5.41E+05
C10H15N2O12	355.062	1.90E+08	C9H16N3O14	390.063	3.36E+06	C19H32N3O20	622.158	1.56E+06	C9H15N2O14	375.052	9.65E+05	C10H16N3O17	450.048	5.35E+05
C10H15N2O13	371.057	1.21E+08	C9H16N2O11	328.075	3.29E+06	C19H31N3O14	525.181	1.54E+06	C20H30N3O18	600.152	9.55E+05	C18H30N2O17	546.154	5.28E+05
C20H32N3O18	602.168	9.13E+07	C20H32N3O13	522.194	3.26E+06	C10H15NO12	341.059	1.53E+06	C19H33N2O15	529.188	9.46E+05	C19H29NO15	511.154	5.12E+05
C10H16N2O13	372.065	8.71E+07	C8H12NO12	314.036	3.21E+06	C10H13N2O12	353.047	1.47E+06	C10H14N3O12	368.058	9.36E+05	C19H32N2O18	576.165	4.89E+05
C10H15N2O14	387.052	4.17E+07	C20H31N2O14	523.178	3.12E+06	C20H31NO16	541.164	1.47E+06	C17H26N3O16	528.131	9.13E+05	C20H31N4O17	599.168	4.89E+05
C20H32N3O16	570.178	3.04E+07	C20H31N2O17	571.162	3.06E+06	C9H14NO7	248.077	1.45E+06	C10H13N2O11	337.052	8.61E+05	C10H15N3O14	401.055	4.73E+05
C9H16N2O12	344.070	2.98E+07	C20H31N2O18	587.157	2.86E+06	C20H30N3O17	584.158	1.45E+06	C20H33N4O21	665.164	8.38E+05	C20H33NO14	511.190	4.66E+05
C20H32N3O15	554.183	2.90E+07	C10H15N2O15	403.047	2.82E+06	C10H16N3O13	386.068	1.37E+06	C8H12N2O12	328.039	8.15E+05	C10H17N2O15	405.063	4.57E+05
C19H30N3O17	572.158	2.58E+07	C19H31N4O15	555.179	2.68E+06	C20H33N4O18	617.179	1.32E+06	C19H32N3O13	510.194	8.09E+05	C9H13N2O9	293.062	4.34E+05
C19H32N3O17	574.173	1.95E+07	C19H30N3O15	540.168	2.58E+06	C7H9N2O13	329.010	1.30E+06	C20H30N3O20	632.142	8.02E+05	C8H11N2O10	295.041	4.04E+05
C10H16N3O15	418.058	1.90E+07	C9H15N2O13	359.057	2.57E+06	C19H28N2O17	556.139	1.28E+06	C18H29N2O14	497.162	7.89E+05	C20H33NO17	559.175	4.01E+05
C10H17N2O12	357.078	1.56E+07	C19H32N3O14	526.188	2.52E+06	C10H14N2O12	354.055	1.27E+06	C19H29NO18	559.138	7.73E+05	C10H17N3O16	435.061	3.75E+05
C9H15N2O11	327.068	1.48E+07	C20H32N3O21	650.153	2.50E+06	C20H30N3O16	568.163	1.27E+06	C10H16N2O16	420.050	7.73E+05	C18H27NO17	529.128	3.55E+05
C10H15N2O11	339.068	1.45E+07	C10H15NO11	325.065	2.44E+06	C18H30N3O17	560.158	1.25E+06	C9H16N3O13	374.068	7.50E+05	C19H33N2O13	497.198	3.52E+05
C19H32N3O15	542.183	1.23E+07	C19H30N3O18	588.152	2.41E+06	C9H5N3O7	267.013	1.24E+06	C9H12N3O13	370.037	7.14E+05	C8H11N2O14	359.021	3.52E+05
C20H33N2O13	509.198	8.74E+06	C9H16N3O12	358.073	2.27E+06	C10H16N3O16	434.053	1.23E+06	C20H31N3O17	585.165	6.65E+05	C19H31N2O20	607.147	3.46E+05
C9H15N2O10	311.073	8.25E+06	C19H32N3O19	606.163	2.19E+06	C9H11N2O11	323.036	1.21E+06	C7H10N2O13	330.018	6.65E+05	C17H26NO16	500.125	2.90E+05
C9H17N2O11	329.083	7.86E+06	C10H15NO15	389.044	2.14E+06	C10H16N3O12	370.073	1.20E+06	C9H13N2O10	309.057	6.62E+05	C7H11N2O11	299.036	2.58E+05
C20H32N3O17	586.173	7.86E+06	C19H31N2O15	527.172	2.03E+06	C9H17N2O12	345.078	1.18E+06	C19H29N2O20	605.131	6.62E+05	C9H12NO8	262.056	2.37E+05
C19H32N3O16	558.178	7.34E+06	C19H30N3O20	620.142	2.01E+06	C20H31N2O21	635.142	1.15E+06	C18H26NO19	560.110	6.59E+05	C10H16NO9	294.083	2.29E+05
C7H9N2O11	297.021	5.67E+06	C10H16N2O15	404.055	1.97E+06	C19H29NO17	543.144	1.14E+06	C19H31N2O12	479.188	6.49E+05	C19H29NO16	527.149	2.26E+05
C19H30N3O14	524.173	5.48E+06	C20H32N3O14	538.188	1.93E+06	C10H14NO11	324.057	1.13E+06	C20H33N2O19	605.168	6.33E+05	C19H34N2O16	546.191	1.70E+05
C20H33N2O16	557.183	5.45E+06	C20H32N2O19	604.160	1.87E+06	C10H16NO11	326.072	1.07E+06	C19H30NO16	528.156	6.29E+05			
C9H14N3O11	340.063	5.18E+06	C10H14NO10	308.062	1.82E+06	C9H14N2O13	358.050	1.03E+06	C9H15N2O9	295.078	6.23E+05			
C10H15NO13	357.054	5.02E+06	C20H32N2O16	556.175	1.81E+06	C10H16NO12	342.067	1.03E+06	C10H16N2O10	324.080	6.23E+05			
C9H15N2O12	343.062	4.92E+06	C20H31N2O15	539.172	1.79E+06	C8H11N3O15	389.019	1.03E+06	C10H14N3O14	400.048	6.20E+05			
C18H30N3O16	544.163	4.37E+06	C10H16N2O14	388.060	1.76E+06	C9H15NO10	297.070	1.01E+06	C10H14N3O13	384.053	6.20E+05			
C19H32N3O18	590.168	4.01E+06	C20H33N2O11	477.208	1.74E+06	C10H16N3O14	402.063	1.01E+06	C9H15N3O16	421.045	6.13E+05			
C10H17N2O13	373.073	3.95E+06	C20H32N3O20	634.158	1.71E+06	C10H14N3O16	432.037	9.98E+05	C9H16N2O13	360.065	5.71E+05			

α -pinene peak list								
HR Peak ID (NO ₃ - cluster)	m/Q	normalized intensity	HR Peak ID (NO ₃ - cluster)	m/Q	normalized intensity	HR Peak ID (NO ₃ - cluster)	m/Q	normalized intensity
NO3	61.988	6.00E+10	C10H15NO12	341.059	6.84E+05	C9H15N2O9	295.078	2.82E+05
HN2O6	124.983	1.89E+10	C20H31N2O16	555.167	6.37E+05	C10H15N3O12	369.066	2.49E+05
H2N3O9	187.979	1.16E+07	C9H11N2O10	307.041	6.17E+05	C10H16N2O16	420.050	2.47E+05
C7H9N2O11	297.021	3.08E+07	C7H10N3O13	344.021	6.04E+05	C9H15N2O11	327.068	2.45E+05
C10H16N2O12	356.070	6.06E+06	C20H31N2O17	571.162	5.79E+05	C10H17N2O12	357.078	2.43E+05
C7H9N2O13	329.010	2.22E+06	C10H15N2O10	323.073	5.46E+05	C20H30NO18	572.146	2.43E+05
C10H14NO12	340.052	1.73E+06	C10H15N2O11	339.068	5.46E+05	C20H32N2O15	540.180	2.37E+05
C18H26NO18	544.115	1.67E+06	C10H16N3O14	402.063	5.46E+05	C19H30N3O16	556.163	2.37E+05
C20H32N3O17	586.173	1.45E+06	C10H14N2O12	354.055	5.36E+05	C9H15N2O12	343.062	1.91E+05
C10H15N2O13	371.057	1.37E+06	C10H14NO10	308.062	5.33E+05	C10H16N3O15	418.058	1.89E+05
C10H15N2O15	403.047	1.36E+06	C9H14N2O15	390.039	5.21E+05	C9H13N2O9	293.062	1.75E+05
C7H10N2O12	314.023	1.31E+06	C10H16N3O13	386.068	5.10E+05	C19H13NO12	447.044	1.75E+05
C10H16N2O14	388.060	1.17E+06	C10H14N3O12	368.058	5.05E+05	C19H30N5O17	600.164	1.70E+05
C10H16N3O17	450.048	1.15E+06	C20H31N2O14	523.178	4.67E+05	C9H14N2O11	326.060	1.32E+05
C9H14N3O13	372.053	1.10E+06	C10H15N2O12	355.062	4.64E+05	C9H12NO9	278.051	1.01E+05
C10H14N3O15	416.042	1.09E+06	C10H14N3O16	432.037	4.58E+05	C10H14NO9	292.067	9.83E+04
C20H32N3O15	554.183	1.06E+06	C10H14NO11	324.057	4.34E+05	C9H12NO8	262.056	8.92E+04
C10H14N2O13	370.050	1.03E+06	C7H10N2O13	330.018	4.09E+05	C10H16NO9	294.083	8.52E+04
C9H14N2O13	358.050	1.02E+06	C10H15N3O15	417.050	4.07E+05	C10H16N2O9	308.086	0.00E+00
C20H32N3O16	570.178	1.00E+06	C10H15N2O14	387.052	3.98E+05	C10H17N3O12	371.081	0.00E+00
C20H32N3O13	522.194	9.55E+05	C20H31N2O18	587.157	3.96E+05			
C9H14N3O15	404.042	9.27E+05	C10H15N3O14	401.055	3.89E+05			
C10H15NO14	373.049	9.12E+05	C10H16N2O10	324.080	3.76E+05			
C20H32N3O14	538.188	8.82E+05	C10H15N3O13	385.060	3.76E+05			
C20H32N3O19	618.163	8.47E+05	C9H13N2O10	309.057	3.53E+05			
C20H32N3O18	602.168	8.41E+05	C10H17N2O14	389.068	3.42E+05			
C7H10N3O11	312.032	7.96E+05	C19H30N2O18	574.149	3.38E+05			
C9H13N2O11	325.052	7.96E+05	C10H14N3O13	384.053	3.20E+05			
C10H15N2O9	307.078	6.97E+05	C20H31N2O20	619.147	2.97E+05			

Figure S12. Peak lists for each MT system